JACS
JOURNAL OF THE AMERICAN CHEMICAL SOCIETY
Communication
pubs.acs.org/JACS

Dual Defects of Cation and Anion in Memristive Nonvolatile Memory of Metal Oxides

Keisuke Oka,[†] Takeshi Yanagida,*[,†,‡] Kazuki Nagashima,[†] Masaki Kanai,[†] Bo Xu,[†] Bae Ho Park,[§] Hiroshi Katayama-Yoshida,[∥] and Tomoji Kawai*[,†,§]

[†]Institute of Scientific and Industrial Research, Osaka University, 8-1 Mihogaoka, Ibaraki, Osaka 567-0047, Japan

[‡]PRESTO, Japan Science and Technology Agency, 4-1-8 Honcho, Kawaguchi, Saitama 332-0012, Japan

[§]Division of Quantum Phases & Devices, Department of Physics, Konkuk University, Seoul 143-701, Republic of Korea

[∥]Department of Materials Engineering Science, Graduate School of Engineering Science, Osaka University, 1-3 Machikaneyama, Osaka 560-8531, Japan

Supporting Information

ABSTRACT: The electrically driven resistance change of metal oxides, called bipolar memristive switching, is a fascinating phenomenon in the development of next-generation nonvolatile memory alternatives to flash technology. However, our understanding of the nature of bipolar memristive switching is unfortunately far from comprehensive, especially the relationship between the electrical transport and the local nonstoichiometry. Here we demonstrate that the coexistence of anion and cation defects is critical to the transport properties of NiO, one of the most promising memristive oxides, by utilizing first-principles calculations. We find that, in the presence of both nickel and oxygen defects, which must exist in any real experimental systems, carrier concentrations of holes generated by nickel defects can be modulated by the presence or absence of oxygen defects around the nickel defect. Such alternation of local nonstoichiometry can be understood in terms of an oxygen ion drift induced by an external electric field. This implication provides a foundation for understanding universally the nature of bipolar memristive switching in various p-type metal oxides.

Memristive switching phenomena at simple metal/oxide/metal junctions have attracted much attention due to not only fundamental interest in the mechanisms but also the potential uses in high-density universal memory devices.[1−6] Memristive switching behaviors can be classified into two types: electrical polarity-dependent (bipolar) and electrical polarity-independent (unipolar).[2] In particular, bipolar memristive switching has been intensively investigated because it offers much more stable memory operations than unipolar switching.[3,4] Among many materials for memristive switching, NiO is one of the most promising due to its high stability and reliable memory characteristics. Many models have been proposed to explain the occurrence of bipolar memristive switching of metal oxides,[5] which have consistently claimed the presence of oxygen vacancies to have an effect on the transport properties. Such oxygen vacancy-based scenarios are clearly applicable for n-type oxides such as TiO_2, because oxygen vacancies act as a donor, while NiO seems to be not ideal for such models because the oxygen vacancy levels in NiO are deep, far from the conduction band.[7−9] In the presence of nickel vacancies, $Ni_{1-x}O$ can be a semiconductor, and the mobile carriers are holes.[10−13] We have also demonstrated the hole-transport nature of bipolar memristive switching behaviors in NiO and CoO by utilizing planar-type nanowire junctions.[14−18] It is noted that, under electric fields, an oxygen ion alone seems to be much more mobile compared with a nickel ion, considering their diffusion constants.[19,20] Therefore, it is necessary to consider a mechanism that explains the occurrence of NiO bipolar switching in terms of the oxygen ion drift rather than the nickel ion drift. This study aims to tackle this essential issue of NiO bipolar memristive switching by studying the transport properties of NiO in the presence of oxygen and nickel vacancies utilizing first-principles calculations (GGA+U). We find that a model based on (1) the coexistence of oxygen and nickel vacancies and (2) the oxygen ion drift under electric field can rigorously explain the occurrence of bipolar switching in NiO. In principle, the model should be applicable to many p-type memristive switching oxides.

Density functional theory calculations were performed with a plane-wave pseudopotential method, as implemented in the QUANTUM-ESPRESSO code.[21] The valence configurations are $3d^8 4s^2$ and $2s^2 2p^4$ for nickel and oxygen, respectively. The Perdew−Burke−Ernzerhof spin-polarized generalized gradient approximation[22] and Hubbard parameter[22] approach (GGA+U) were utilized to determine the exchange and correlation energies of electrons and on-site Coulomb correction. We used 8.5 eV for Hubbard parameter U as a simplified rotationally invariant form of the Hubbard term.[24] The energy cutoffs for wave functions and charge density are 54 and 218 eV. The *k*-point 4×4×4 regular mesh in the Monkhorst−Pack grid[24] was used. The number of atoms in the supercell is 64 ($Ni_{32}O_{32}$), giving a simple cubic cell with antiferromagnetic structure, as shown in Figure 1a. To calculate defect states including anion and cation vacancies, one nickel atom and one oxygen atom were removed from the supercell, respectively, and also the number of electrons was adjusted according to removed atoms

Received: December 7, 2011
Published: January 20, 2012

dx.doi.org/10.1021/ja2114344 | J. Am. Chem.Soc. 2012, 134, 2535−2538

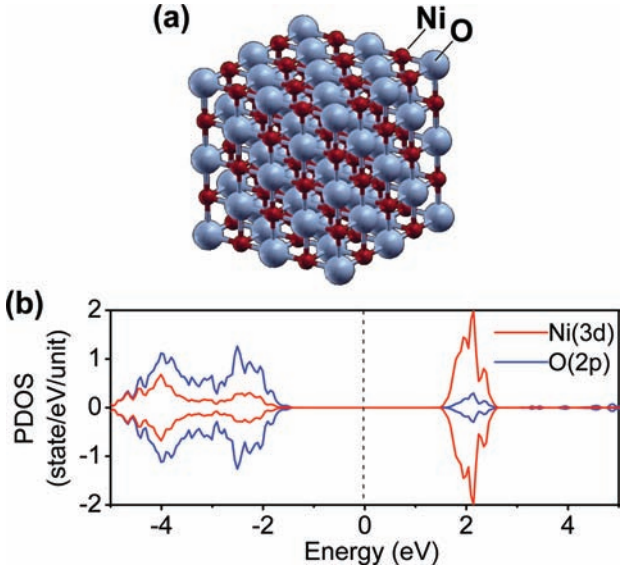

Figure 1. (a) Supercell ($Ni_{32}O_{32}$) geometry of a simple cubic style. The length of the lattice vector is 8.354 Å. (b) PDOS of defect-free NiO. The Fermi level is centered between the valence band maximum and the conduction band maximum as 0 eV. The red and blue lines show Ni 3d and O2p, respectively.

to give a neutral charge state. The atomic positions for structural optimization are relaxed with the damped dynamics (quick-min Verlet)[26] algorithm. The density of states (DOS) is broadened by the Gaussian function with a width of 0.05 eV. The partial density of states (PDOS) is plotted as the sum nickel 3d and oxygen 2p orbitals in the supercell. The Fermi level is set to 0 eV.

First, we calculated the electric structure of stoichiometric NiO without any vacancies, and the calculated PDOS is shown in Figure 1b. The magnetic moment of one nickel ion and the energy gap are calculated to be 1.8 μ_B and 3 eV, respectively, in good agreement with experimental results and also previous calculations using GGA+U.[8,27−30] Figure 1b shows high orbital hybridization between nickel 3d and oxygen 2p orbitals at the valence band maximum (VBM), which is closely related to a superexchange interaction between up-spin and down-spin of the nickel ion-mediated oxygen 2p orbital. On the other hand, the states at the conduction band minimum (CBM) are composed of nickel 3d orbitals. These results indicate that the calculated electric structure of NiO is a charge-transfer type.[9] The effects of oxygen vacancy or nickel vacancy on the PDOS are calculated to reveal the effect of nonstoichiometry on the electrical conductivity of NiO. Figure 2a,b shows the calculated PDOS data in the presence of oxygen vacancy or nickel vacancy. Compared with the PDOS of stoichiometric NiO in Figure 1b, each vacancy forms significant defect states within the band gap between the VBM and CBM. Nickel vacancies form the defect states near the VBM, whereas oxygen vacancies form the defect states at deep energy levels far from the VBM and CBM, as shown in Figure 2b. Considering these trends, in the presence of oxygen vacancies, electrons seem to be highly localized because of the absence of unoccupied DOS near the Fermi level. On the other hand, in the presence of nickel vacancies, hole carriers can be generated by the defect states near the VBM. This calculation result supports an experimental trend that NiO with nickel vacancies is a p-type semiconductor. Figure 2c shows the calculated PDOS in the coexistence of

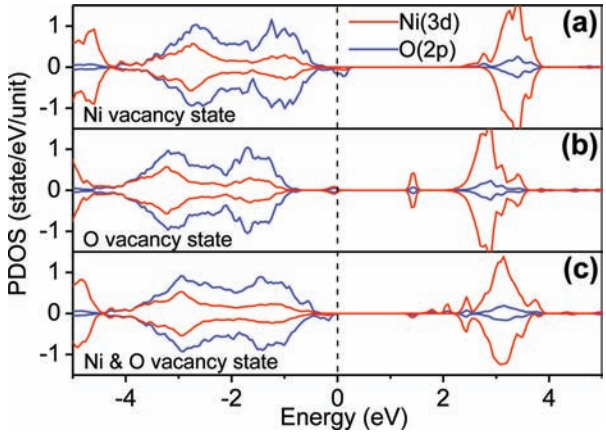

Figure 2. PDOS consisting of (a) nickel vacancy, (b) oxygen vacancy, and (c) coexistence of nickel and oxygen vacancies. The Fermi level is set to 0 eV. The red and blue lines show Ni 3d and O2p, respectively.

oxygen and nickel vacancies, where the nickel vacancy is located at the nearest neighbor of oxygen vacancy. It can be seen that the PDOS near the Fermi level decreases upon introducing oxygen vacancy around nickel vacancy, highlighting that the existence of oxygen vacancy strongly affects the defect states formed by nickel vacancy.

Since the above calculations assume the nearest-neighbor pair of oxygen and nickel vacancies, we examine the effect of the distance between nickel and oxygen vacancies. Figure 3

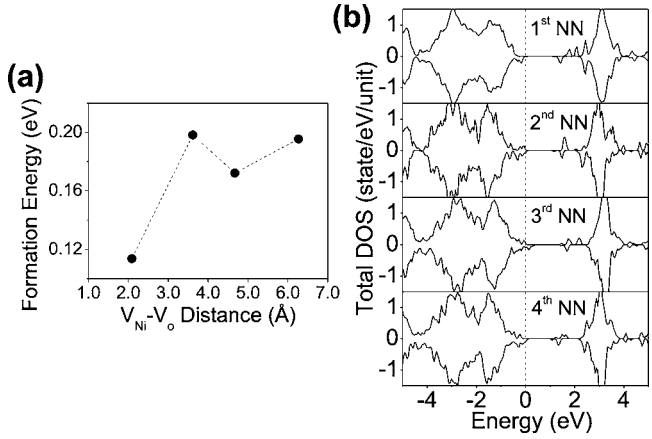

Figure 3. (a) Correlation between formation energy and distance between coexisting nickel and oxygen vacancies. (b) Total DOS when varying the distance between nickel and oxygen vacancies.

shows the formation energy of coexisting states, which depends on the distance between nickel and oxygen vacancies. The formation energy E_{form} is here defined by the following formula: $E_{form} = E_{tot}(V_{Ni}=N_{Ni},V_O=N_O) - E_{tot}(V_{Ni=O},V_{O=O} + N_{Ni}E_{tot}(Ni\text{-}(fcc)) + N_OE_{tot}(O_2)/2$, where E_{tot} is the total energy of a supercell, V_{Ni} is a nickel vacancy, N_{Ni} is the number of nickel vacancies, V_O is an oxygen vacancy, N_O is the number of oxygen vacancies, $E_{tot}(Ni(fcc)$ is the total energy of metal nickel (face-centered cubic), and $E_{tot}(O_2)$ is the total energy of an oxygen molecule. The calculations indicate that the nearest-neighbor pair of vacancies is most stable in the presence of coexisting nickel and oxygen vacancies in NiO.

To understand the effect of the coexistence of these vacancies on the DOS, we focus on the microscopic origin of

dx.doi.org/10.1021/ja2114344 | J. Am. Chem.Soc. 2012, 134, 2535−2538

the defect states near the VBM in the presence of vacancies. Figure 4a shows the calculated charge density spatial

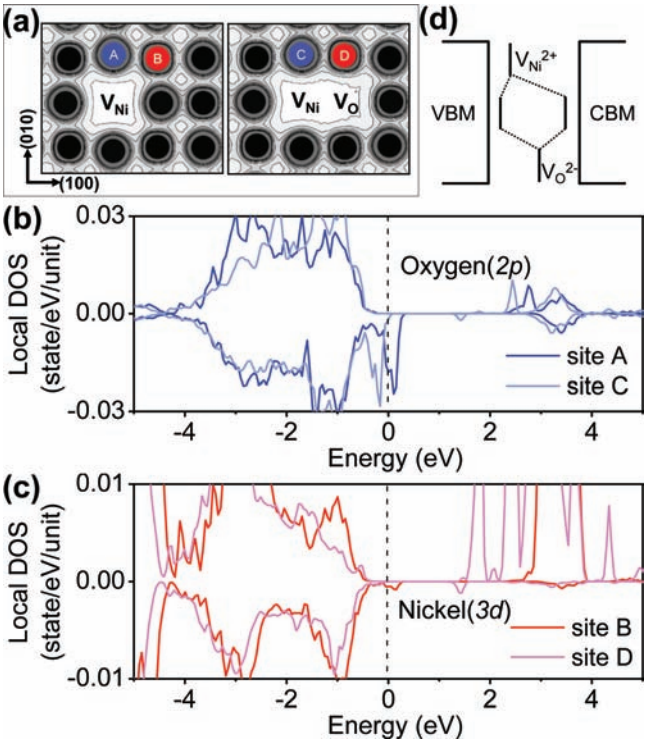

Figure 4. (a) Mapping the charge density distribution on a single defect state of nickel (left) and coexisting defects states of nickel and oxygen (right). (b) LDOS on oxygen ion sites A and C with 2p orbitals (solid line). (c) LDOS on nickel ion sites B and D with 3d orbitals (dashed line). (d) Schematic energy diagram when pairing an oxygen vacancy and a nickel vacancy.

distribution on the single nickel vacancy and/or the coexistence of nickel and oxygen vacancies. Figure 4b,c compares the single nickel vacancy and the coexistence of nickel and oxygen vacancies on the local density of state (LDOS) at oxygen ion sites (A and C in Figure 4a) and those at nickel ion sites (B and D in Figure 4a). It can be seen that the presence of an oxygen vacancy near a nickel vacancy strongly suppresses the LDOS near the Fermi level. In principle, making a pair of two states (in this case, pairing oxygen and nickel vacancies) creates the bonding and antibonding states from two isolated states, which lowers one state's energy and increases the other state's energy in the heterogeneous pairing. The presence of such bonding and antibonding states can be seen in the calculated PDOS and LDOS in Figures 2c and 4b,c. In this case, when introducing an oxygen vacancy around a nickel vacancy, the nickel vacancy energy level is lowered, whereas the oxygen vacancy state shifts to a higher energy level, as shown in Figure 4d. In this case, the Fermi level lies somewhere between the two states because charge neutrality requires electrons to fill the nickel vacancies, which decreases the unoccupied DOS near the Fermi level. We have also examined the effect of lattice relaxation on the PDOS, as shown in Figure 5. The calculated result indicates that the lattice relaxation around a nickel vacancy plays a major role in suppressing the PDOS at the Fermi level.

These calculated results highlight that the transport properties of NiO can be modulated by the amount of oxygen vacancies around the nickel vacancies. This implication is quite

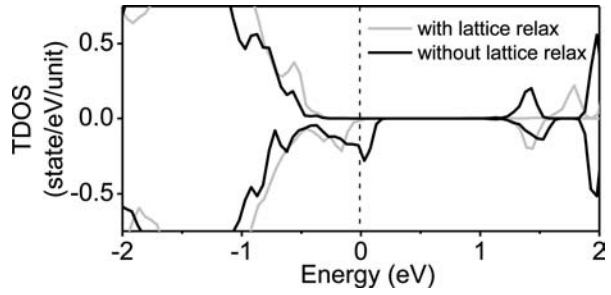

Figure 5. Effect of lattice relaxation on total DOS near the Fermi level in the case of coexistence of oxygen and nickel vacancies.

important to understanding the nature of bipolar memristive switching, because an oxygen ionic drift can alter the electrical conductivity of NiO, even without the movements of nickel vacancies. This is in sharp contrast with previous implications based on only oxygen vacancy-based models. In addition, the coexistence of anion and cation vacancies rather than only one element vacancy[29,30] must be realistic in any experimental NiO systems. Based on the theoretical calculations in the presence of both oxygen and nickel vacancies, the bipolar memristive switching behaviors of NiO can be interpreted as follows. Applying an external electric field drives a drift of oxygen ions toward the positively charged (anode) electrode above the critical electric field.[31] Such oxygen ion drift increases the concentration of isolated nickel vacancies near the anode side, as shown in Figures 2 and 4. The spatial position near the anode side is then more conductive than in the pristine sample due to the increased concentration of isolated nickel vacancies. This conductive region can be extended from the anode to the cathode as a conducting path. The conductive region finally is in contact with the other side electrode—cathode, and then the memristive switching (called a single-electron-transfer process from OFF to ON states) occurs. The inversed RESET process from ON to OFF states occurs via disconnecting the thinnest point of path near the original cathode via a drift of oxygen ions. Thus, this model infers the occurrence of bipolar memristive switching in NiO at the cathode side, which is consistent with our previous experimental results.[19,20] Note that this cathode-side switching of NiO is in sharp contrast with bipolar memristive switching of n-type oxides, in which the memristive switching occurs at the anode side.[32]

In summary, we have demonstrated the crucial role of the coexistence of anion and cation defects in determining the transport properties of nonstoichiometric NiO by utilizing first-principles calculations. We found that, in the presence of both nickel and oxygen defects, which must exist in any real experimental systems, carrier concentrations of holes, which are generated from acceptor levels formed by nickel defects, can be modulated by the presence or absence of oxygen defects around nickel defects. Such alternation of local nonstoichiometry could be understood in terms of an oxygen ion drift induced by an external electric field. This implication is in sharp contrast with existing models based on only oxygen defects and provides a foundation for understanding the nature of bipolar memristive switching in various p-type oxides.

■ ASSOCIATED CONTENT

Supporting Information

Complete refs 4 and 21. This material is available free of charge via the Internet at http://pubs.acs.org.

dx.doi.org/10.1021/ja2114344 | J. Am. Chem.Soc. 2012, 134, 2535−2538

AUTHOR INFORMATION

Corresponding Author

yanagi32@sanken.osaka-u.ac.jp; kawai@sanken.osaka-u.ac.jp

Notes

The authors declare no competing financial interest.

ACKNOWLEDGMENTS

This work was supported by NEXT Project. T.K. and B.H.P. were partly supported by WCU program (Grant No. R31-2008-000-10057-0). T.K. was supported by FIRST.

REFERENCES

(1) Strukov, D. B.; Williams, R. S. *Proc. Natl. Acad. Sci. U.S.A.* **2009**, *106*, 20155.
(2) Waser, R.; Aono, M. *Nat. Mater.* **2007**, *6*, 833.
(3) Lee, M. J.; Lee, C. B.; Lee, D.; Lee, S. R.; Chang, M.; Hur, J. H.; Kim, Y. B.; Kim, C. J.; Seo, D. H.; Seo, S.; Chung, U. I.; Yoo, I. K.; Kim, K. *Nat. Mater.* **2011**, *10*, 625.
(4) Lee, M. J.; et al. *Adv. Mater.* **2008**, *20*, 924.
(5) Waser, R.; Dittmann, R.; Staikov, G.; Szot, K. *Adv. Mater.* **2009**, *21*, 2632.
(6) Pershin, Y. V.; Di Ventra, M. *Adv. Phys.* **2009**, *60*, 145.
(7) Cho, E.; Han, S.; Ahn, H. S.; Lee, K. R.; Kim, S. K.; Hwang, C. S. *Phys. Rev. B* **2006**, *73*, 193202.
(8) Park, S.; Ahn, H. S.; Lee, C. K.; Kim, H.; Jin, H.; Lee, H. S.; Seo, S.; Yu, J.; Han, S. *Phys. Rev. B* **2008**, *77*, 134103.
(9) Sawatzky, G. A.; Allen, J. W. *Phys. Rev. Lett.* **1984**, *53*, 2339.
(10) Bosman, A. J.; Crevecoe, C *Phys. Rev.* **1966**, *144*, 763.
(11) Lee, M. H.; Kim, K. M.; Kim, G. H.; Seok, J. Y.; Song, S. J.; Yoon, J. H.; Hwang, C. S. *Appl. Phys. Lett.* **2010**, *96*, 152909.
(12) Kinoshtia, K.; Okutani, T.; Tanaka, H.; Hinoki, T.; Yazawa, K.; Ohmi, K.; Kishida, S. *Appl. Phys. Lett.* **2010**, *96*, 143505.
(13) Yoshida, C.; Kinoshita, K.; Yamasaki, T.; Sugiyama, Y. *Appl. Phys. Lett.* **2008**, *93*, 042106.
(14) Oka, K.; Yanagida, T.; Nagashima, K.; Tanaka, H.; Kawai, T. *J. Am. Chem. Soc.* **2009**, *131*, 3434.
(15) Oka, K.; Yanagida, T.; Nagashima, K.; Kawai, T.; Kim, J. S.; Park, B. H. *J. Am. Chem. Soc.* **2010**, *132*, 6634.
(16) Nagashima, K.; Yanagida, T.; Oka, K.; Taniguchi, M.; Kawai, T.; Kim, J. S.; Park, B. H. *Nano Lett.* **2010**, *10*, 1359.
(17) Nagashima, K.; Yanagida, T.; Oka, K.; Kanai, M.; Klamchuen, A.; Kim, J. S.; Park, B. H.; Kawai, T. *Nano Lett.* **2011**, *11*, 2114.
(18) Oka, K.; Yanagida, T.; Nagashima, K.; Kanai, M.; Kawai, T.; Kim, J. S.; Park, B. H. *J. Am. Chem. Soc.* **2011**, *133*, 12482.
(19) Volpe, M. L.; Reddy, J. *J. Chem. Phys.* **1970**, *53*, 1117.
(20) Atkinson, A. *Rev. Mod. Phys.* **1985**, *57*, 437.
(21) Giannozzi, P.; et al. *J. Phys. Condens. Mat.* **2009**, *21*, 359902.
(22) Perdew, J. P.; Burke, K.; Ernzerhof, M. *Phys. Rev. Lett.* **1996**, *77*, 3865.
(23) Anisimov, V. I.; Zaanen, J.; Andersen, O. K. *Phys. Rev. B* **1991**, *44*, 943.
(24) Cococcioni, M.; de Gironcoli, S. *Phys. Rev. B* **2005**, *71*, 035105.
(25) Monkhorst, H. J.; Pack, J. D. *Phys. Rev. B* **1976**, *13*, 5188.
(26) Arias, T. A.; Payne, M. C.; Joannopoulos, J. D. *Phys. Rev. B* **1992**, *45*, 1538.
(27) Cheetham, A. K.; Hope, D. A. O. *Phys. Rev. B* **1983**, *27*, 6964.
(28) Dudarev, S. L.; Botton, G. A.; Savrasov, S. Y.; Humphreys, C. J.; Sutton, A. P. *Phys. Rev. B* **1998**, *57*, 1505.
(29) Han, S.; Park, S.; Ahn, H. S.; Lee, C. K.; Kim, H.; Jin, H.; Lee, H. S.; Seo, S.; Yu, J. *Phys. Rev. B* **2008**, *77*, 134103.
(30) Lee, H. D.; Magyari-Kope, B.; Nishi, Y. *Phys. Rev. B* **2010**, *81*, 193202.
(31) Strukov, D. B.; Williams, R. S. *Appl. Phys. A, Mater.* **2009**, *94*, 515.
(32) Szot, K.; Speier, W.; Bihlmayer, G.; Waser, R. *Nat. Mater.* **2006**, *5*, 312.